ChemComm

COMMUNICATION

View Article Online
View Journal | View Issue

Cite this: *Chem. Commun.*, 2019, 55, 14434

Received 12th September 2019,
Accepted 12th November 2019

DOI: 10.1039/c9cc07150d

rsc.li/chemcomm

Supramolecular chirogenesis in zinc porphyrins by enantiopure hemicucurbit[*n*]urils (*n* = 6, 8)†

Lukas Ustrnul, [a] Sandra Kaabel, [a] Tatsiana Burankova,[b] Jevgenija Martõnova,[a] Jasper Adamson, [c] Nele Konrad,[a] Peeter Burk, [d] Victor Borovkov *[ae] and Riina Aav *[a]

Chiral cyclohexanohemicucurbit[*n*]urils (*n* = 6, 8) (cycHCs) are able to bind guests through multiple "outer surface interactions", which in the case of planar zinc porphyrins leads to induction of chirality. Crystal structures of complexes of complementary sized hosts revealed social self-sorting, while in the solution phase one cycHC can accommodate up to three porphyrin molecules with log K_{total} 9.

Porphyrins are a special group of aromatic tetrapyrrolic compounds possessing unique spectroscopic properties. They are extensively used in a broad range of various applications, *e.g.*, catalysis,[1,2] building blocks for MOFs and artificial molecular machines,[2–4] diagnostics and photodynamic therapy,[5] chemical sensing,[6] and recognition of chiral molecules.[7–9] There are two basic strategies for their chiral applications: (1) employing covalently modified chiral porphyrins and (2) supramolecular chirogenesis, which is based on the asymmetry transfer from a chiral guest molecule to porphyrin(s) *via* noncovalent interactions.[10] Such a chirogenic process leads to induced circular dichroism (ICD) in the region of porphyrin absorption. In general, the ICD intensity of porphyrin molecules is more prominent if several porphyrin units are involved[7,8,11] and rather moderate for monomeric porphyrins either in organic[12,13] or aqueous solutions.[14–16] Nevertheless, porphyrin aggregates formed in aqueous media also exhibit intense ICD signals.[17–24]

Chiral macrocycles, cyclohexanohemicucurbit[*n*]urils (**cycHC[6]** and **cycHC[8]**, see Fig. 1A), have complementary dimensions with porphyrins, with their height being close to a nanometer.[25–27] They are easily accessible[25,27] and have the ability to bind carboxylic acids enantioselectively.[25,27] The main feature of the larger **cycHC[8]** is the selective binding of anions inside the cavity, governed by the size, shape, and charge distribution of the guest.[28] While anion binding is widely studied for the whole family of hemicucurbiturils,[29] the external binding to polar urea moieties has received much less attention. The study by Buschmann[30] and some crystallographic evidence showed the coordination of thiophilic cations, Pd^{2+} and Hg^{2+}, to the thiourea moiety of thiobambus[4]uril[31] and Na^{+} cation interaction with the carbonyl oxygen of biotin[6]uril.[32]

Herein, we present the first example of chirality transfer from (*R*,*R*)- and (*S*,*S*)-enantiomers of **cycHC[6]** and **cycHC[8]** to achiral zinc octaethylporphyrin (**ZnOEP**) and zinc tetraphenylporphyrin (**ZnTPP**) (Fig. 1A) upon the supramolecular "outer surface interactions", studied in solution and in the solid phase. The ability of **cycHC[6]** to imprint its chirality into achiral **ZnTPP** was investigated using circular dichroism in a nonpolar solvent and simulated computationally (Fig. 1B, C, and ESI†).

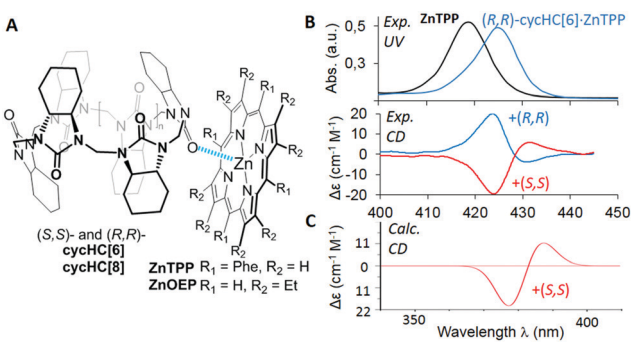

Fig. 1 (A) Structures of studied complexes; (B) UV-vis and CD spectra of **ZnTPP** and its complexes with (*S*,*S*)-**cycHC[6]** and (*R*,*R*)-**cycHC[6]** in DCM; (C) TD-DFT simulated spectrum of **ZnTPP**·(*S*,*S*)-**cycHC[6]** complex. (See ESI† for details).

[a] *Department of Chemistry and Biotechnology, Tallinn University of Technology, Akadeemia tee 15, 12618 Tallinn, Estonia. E-mail: riina.aav@taltech.ee*
[b] *Paul Scherrer Institute, Laboratory for Neutron Scattering and Imaging, Forschungsstrasse 111, 5232 Villigen PSI, Switzerland*
[c] *National Institute of Chemical Physics and Biophysics, Akadeemia tee 23, 12618 Tallinn, Estonia*
[d] *Faculty of Science and Technology, University of Tartu, Vanemuise 46-208, 51014 Tartu, Estonia*
[e] *College of Chemistry and Materials Science, South-Central University for Nationalities, 182# Minzu RD, Hongshan District, Wuhan, Hubei Province 430074, China. E-mail: victor.borovkov@scuec.edu.cn*

† Electronic supplementary information (ESI) available. CCDC 1949778 and 1949779. For ESI and crystallographic data in CIF or other electronic format see DOI: 10.1039/c9cc07150d

The addition of (*S*,*S*)-**cycHC[6]** to a dichloromethane (DCM) solution of **ZnTPP** resulted in the bathochromic shift of porphyrin absorption maxima up to 425 nm and the appearance of positive and negative Cotton effects in the region of the porphyrin Soret band at 431 and 424 nm, respectively (Fig. 1B).

The sole role of hemicucurbituril chirality in the ICD of **ZnTPP** was confirmed by employing antipodal **cycHC[6].** Hence, (*R*,*R*)-**cycHC[6]** induced a perfect mirror image CD spectrum of **ZnTPP**. The CD spectra of other combinations of **cycHCs** and porphyrins; (*S*,*S*)/(*R*,*R*)-**cycHC[6]·ZnOEP**, (*S*,*S*)/(*R*,*R*)-**cycHC[8]·ZnOEP**, and (*S*,*S*)/(*R*,*R*)-**cycHC[8]·ZnTPP** gave similar results (Fig. S1–S4, ESI†), thus, confirming the generality of the chirogenic mechanism. The CD spectra were recorded in the presence of an excess of **cycHCs**, and therefore 1 : 1 complex formation was assumed. To probe the ICD ability of the monomeric unit of **cycHCs**, (*R*,*R*)-*N*,*N*′-dimethyl- and (*R*,*R*)-*N*,*N*′-diphenyl-cyclohexadiylurea (**M1**, **M2**) were used in a similar manner exhibiting no appreciable ICD in **ZnTPP** (Fig. S6, ESI†), pointing to differences in binding character of **cycHCs** compared with mono-ureas.

For unambiguous rationalization of the mechanism of chirality transfer and the mode of interaction of **cycHCs** with porphyrins, the corresponding time-dependent density functional theory (TD-DFT) simulation of **cycHC[6]·ZnTPP** complex was performed. The calculated CD spectrum of **cycHC[6]·ZnTPP** gave very good agreement with the experimental data (Fig. 1C), confirming the presence of 1 : 1 stoichiometry in the complex. The optimized geometry revealed the strongest interaction site between the porphyrin Zn cation and urea carbonyl of **cycHC**, with the Zn···O=C distance being 2.203 Å. Localization of the highest occupied molecular orbital (HOMO) depicted in Fig. 2 shows distortion of porphyrin ring planarity that appears to be a prime cause of the chirality transfer mechanism. See ESI† for other orbitals involved in the electronic transitions.

We were fortunate to grow single crystals of the **cycHC[6]** and **cycHC[8]** complexes with **ZnTPP** (Fig. 3). Both the crystallographic structures showed distortion of the porphyrin plane in comparison to the planar conformation of noncomplexed porphyrin. The crystallographic structure of **cycHC[6]·ZnTPP** (Fig. 3A) revealed a rather unusual mode of binding with hexacoordinative zinc porphyrin forming a supramolecular linear chain with the **cycHC[6]** macrocycle and resulting in the overall 1 : 1 **cycHC[6]·ZnTPP** stoichiometry. Indeed, while zinc porphyrins are generally pentacoordinative in solution, several crystal structures of six-coordinated zinc porphyrins have been reported in the literature.[33–37] Mostly, they are formed by self-association, however, there is one particular example of **ZnTPP** complexed with two tetrahydrofuran molecules.[38] In addition, two examples of solution-phase studies of six-coordinated zinc porphyrin derivatives, utilizing chelate effect while coordinated to the Zn atom by heteroaromatic nitrogens, have been reported.[39,40] In the case of **cycHC[6]·ZnTPP** complex, the average length of Zn···O is 2.39 Å, which is similar to other six-coordinated zinc complexes. Furthermore, the π-system of **ZnTPP** interacts with multiple C–H groups originating from the methylene bridges and cyclohexano moieties of **cycHCs**. The distances between the **cycHC[6]** hydrogens and the porphyrin mean plane are as follows: 2.39–2.66 Å for the methylene bridge and 2.64–3.10 Å for the cyclohexano group. Interestingly, the interacting protons of cyclohexano moieties are not of the urea subunit coordinated on the metal center but belong to the adjacent urea subunits. This observation suggests that the lack of these additional interactions with mono-urea derivative **M1** allows free rotation around the coordination bond resulting in negligible ICD (see ESI†). At the same time, it emphasizes the appropriate preorganization of **cycHCs**' shape allowing multiple-point interactions with porphyrins.

In contrast, the crystal structure of **cycHC[8]·ZnTPP** shows the 1 : 2 complexation where one molecule of **cycHC[8]** is surrounded by four molecules of porphyrin with only two of them being complexed. Moreover, the two interacting porphyrins are bound pincer-like to the aligned urea subunits (Fig. 3B) separated by a single alternate monomer. However, the intermolecular interactions in crystals of **cycHC[8]·ZnTPP** are similar to those described for the **cycHC[6]** complexes.

The Zn···O=C distance between the porphyrin and macrocycle moieties is 2.17 Å in **cycHC[8]** crystals, showing a larger overlap of van der Waals radii compared with the **cycHC[6]·ZnTPP** crystal. Besides, each porphyrin is also attached to **cycHC[8]** *via* a set of the C–H···π interactions with the strongest one found for the methylene bridge protons, where the distance from the porphyrin mean plane is 2.23–2.86 Å. In addition, weak interaction can be assumed for some of the protons of the cyclohexano group. These crystallographic structures revealed that the main attractive interaction occurs between the zinc cation of porphyrin and carbonyl oxygen of **cycHCs**, hence having six and eight potential binding sites in **cycHC[6]** and **cycHC[8]**, respectively. However, it is sterically impossible for the porphyrins to be simultaneously attached to the neighboring monomeric units of **cycHCs**. Therefore, based on the crystallographic structures obtained, it is reasonable to assume that in the solution phase bulky **cycHC[6]** and **cycHC[8]** might be able to accommodate up to three and four porphyrin molecules, respectively.

The stoichiometry of the **cycHC[6]·ZnTPP** complex in DCM solution was explored using a ^{1}H NMR Job plot (Fig. S35, ESI†). Although this method is only indicative as was shown by Jurczak *et al.*,[41] the results showed the existence of the complex with a stoichiometry higher than **cycHC[6] : ZnTPP** 1 : 2. Moreover, it is reasonable to suggest that the stability of subsequent complexations is decreased with increasing the stoichiometry ($K_1 \geq K_2 \geq K_3 \geq K_4$) as a result of lowering the number of accessible binding sites. To characterize the binding and to

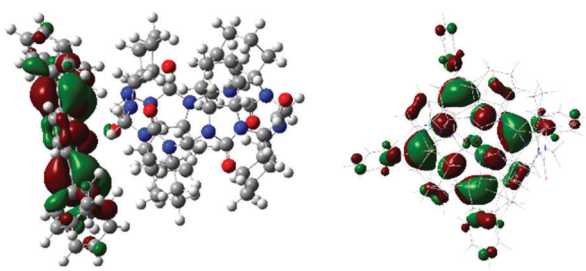

Fig. 2 Visualization of the HOMO orbital of (*S*,*S*)-**cycHC[6]·ZnTPP**.

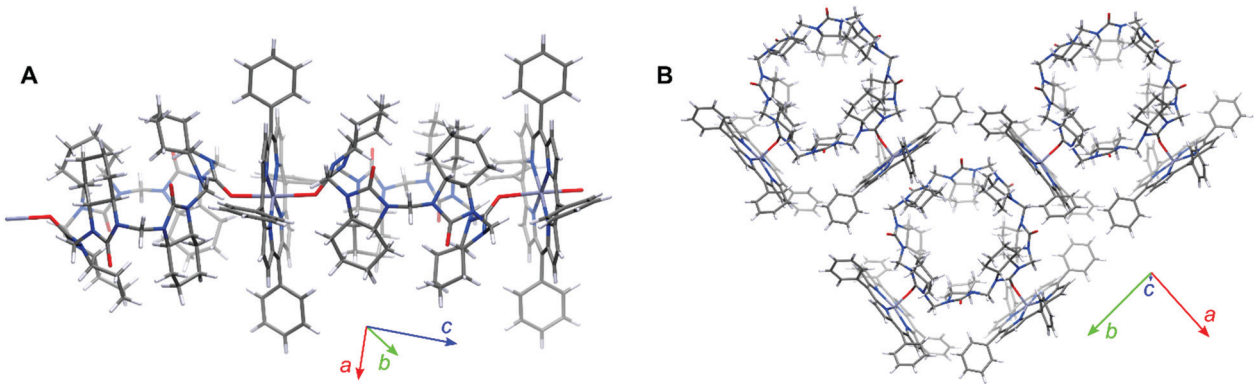

Fig. 3 Single-crystal structure of (A) 1 : 1 1D polymer of (*R*,*R*)-**cycHC[6]·ZnTPP**, (B) 1 : 2 complex of (*R*,*R*)-**cycHC[8]·ZnTPP**. The solvent molecules have been omitted for clarity. Element colors: C gray, N blue, O red, H white, Zn light blue.

evaluate the association constants of **cycHC**–porphyrin complexes in the solution phase, UV-vis and ^{1}H NMR titration experiments were carried out. Because there is no commonly available tool for the calculation of 1 : 3 and 1 : 4 binding equilibria, we developed our own script for the analysis of this specific system. While a 1 : 4 binding model for the **cycHC[8]**-based systems appeared to be too overparameterized to deliver stable results, a simpler 1 : 3 model was used for all systems studied. We suppose that this simplification has a minor impact on the obtained values because the K_4 value is expected to be small in comparison to K_1, K_2, and K_3 and the abundance of 1 : 4 complex is negligible. We focused on the **cycHC[8]·ZnTPP** complex as a representative example because it can be additionally utilized for anion binding.[28] Thus, data from four UV-vis and three NMR titrations, covering the 0.6–5000 μM concentration range of **ZnTPP** were collected. Independent fitting of these data resulted in similar stepwise decreasing association constants; $K_1 > K_2 > K_3$ (Table 1, see ESI† for fitting methodology). In addition, two isothermal titration calorimetry (ITC) experiments have been carried out and analyzed in terms of the sequential binding model, while the initial values for fitting were the association constants obtained from the UV-vis and NMR titrations. Thermodynamic parameters obtained using ITC indicated the independence of the binding sites, with very close values of binding enthalpies for each individual binding step (Table 1). In addition, these experiments unambiguously confirmed the initial assumption that $K_1 \geq K_2 \geq K_3$. It must be noted that fairly strong total external binding constants can be reached due to the multiple site binding (Table 1).

Table 1 Stepwise association constants; K_1, K_2, K_3 for the 1 : 3 binding model[a] of **cycHC[8]·ZnTPP** obtained in DCM solutions by NMR, UV-vis, and ITC methods and their thermodynamic parameters ΔH and $T\Delta S$ obtained from ITC at 293 K

No.		K_1 (M^{-1})	K_2 (M^{-1})	K_3 (M^{-1})	log K_{total}[b]
1	NMR	1890 ± 60	1100 ± 80	50 ± 25	8.02
2	UV-vis	2070 ± 20	900 ± 20	430 ± 120	8.90
3	ITC	2280 ± 150	770 ± 20	400 ± 20	8.84
4	ΔH (kJ mol^{-1})	−24.0 ± 0.15	−26.8 ± 0.5	−28.0 ± 0.4	
5	$T\Delta S$ (kJ mol^{-1})	−5.1 ± 0.6	−10.5 ± 0.5	−13.4 ± 0.4	

[a] $K_n = \frac{[\text{cycHC} \cdot \text{ZnP}_n]}{[\text{cycHC} \cdot \text{ZnP}_{n-1}] \cdot [\text{ZnP}]}$, where ZnP is Zn–porphyrin and n is stoichiometry. [b] $K_{total} = K_1 \cdot K_2 \cdot K_3$.

Table 2 Association constants K_1 (M^{-1}) calculated according to the 1 : 3 binding model for **cycHCs** complexes and according to 1 : 1 binding model for **M1** in DCM solutions

		Titration method	
No.	Complex	NMR	UV-vis
1	**cycHC[6]·ZnTPP**	5000 ± 200[a]	5340 ± 60
2	**cycHC[6]·ZnOEP**	4200 ± 130[b]	3070 ± 30
3	**cycHC[8]·ZnTPP**[c]	1890 ± 60	2070 ± 20
4	**cycHC[8]·ZnOEP**	705 ± 18	880 ± 20
5	**M1·ZnTPP**[d]	50.5 ± 0.8	57.4 ± 1.1
6	**M1·ZnOEP**[d]	—	12.4 ± 0.3

[a] From three titrations obtained also K_2 = 1900 ± 200 M^{-1}, K_3 = 190 ± 16 M^{-1}. [b] In addition, K_2 = 950 ± 40 M^{-1} obtained. [c] For all K_n see Table 1. [d] Results evaluated using the 1 : 1 model from http://supramolecular.org.

Because the binding mechanism for all supramolecular systems studied is essentially the same, just a comparison of the corresponding K_1 values is sufficient to evaluate the complex stability. Therefore, other **cycHCs** and Zn–porphyrin complexes were studied to an extent necessary to obtain the K_1 values (Table 2). In addition, the K_1 values for mono-urea **M1** and porphyrins were determined using the 1 : 1 binding model[42,43] to reveal approximately 100 times weaker interaction in comparison to **cycHCs**. Bulkier **M2** provided negligible binding (Fig. S22, ESI†). Analogous observations were made earlier by us in the study of external binding of a Brønsted acid to **cycHC[6]s** and **M1**.[44] The significantly lower external binding between **M1** and Zn–porphyrins is assumed to be caused by the lack of multiple-point interaction. A general trend in the stability of complexes is as follows: **cycHC[6]·ZnTPP** > **cycHC[6]·ZnOEP** > **cycHC[8]·ZnTPP** > **cycHC[8]·ZnOEP** ≫ **M1·ZnTPP** > **M1·ZnOEP**. The higher stability of **ZnTPP** over **ZnOEP** complexes clearly reflects the dependence of binding upon the electron-accepting ability of the Zn ion as a result of the presence of Ph groups in **ZnTPP**. The stability of **cycHC[6]** complexes over the **cycHC[8]** is not so evident and needs further investigations. Apparently, the clear differences in binding six and eight membered **cycHC** homologues in solution and solid phase reflect the strong influence of geometry on their interaction mode.

In conclusion, for the first time, we demonstrated that zinc porphyrins can be effectively used to sense hemicucurbituril chirality. The used macrocycles have large association constants with porphyrins thanks to their suitable preorganization. The main interaction point is coordination between the electron-deficient porphyrin zinc ion and electron-rich carbonyl oxygen on the outer part of **cycHCs**. The collected data fully support the 1 : 3 **cycHC** : porphyrin stoichiometry as the major complexation process in solution. Chiroptical studies indicated an efficient chirality transfer process from chiral **cycHCs** to achiral zinc porphyrins *via* a chiral ring distortion mechanism. The observed chirogenic phenomenon opens further prospects to utilize the **cycHCs**'s cavity available for another guest molecule to modulate induced chirality by formation of more complexed supramolecular systems and other molecular networks for sensing and/or catalytic applications.

The authors acknowledge Mohammed Hasan, Kamini Mishra, Karina Barsunova, Aleksandra Gluškova, Tatsiana Shalima, and Paul Kerner for experimental assistance and Pall Thordarson for useful discussions. We also thank the Estonian MER for financial support through Grants PUT692, PRG399, IUT 19-9; the ERDF through the CoE 3.2.0101.08-0017, CoE 2014- 2020.4.01.15-0013, CoE TK134; the H2020-FETOPEN, 828779 (INITIO); and the start-up research grant YZZ16005 from South-Central University for Nationalities; as well as the High-Performance Computing Center of the University of Tartu.

Conflicts of interest

There are no conflicts to declare.

Notes and references

1 H. Lu and X. P. Zhang, *Chem. Soc. Rev.*, 2011, **40**, 1899–1909.
2 J. Lee, O. K. Farha, J. Roberts, K. A. Scheidt, S. T. Nguyen and J. T. Hupp, *Chem. Soc. Rev.*, 2009, **38**, 1450–1459.
3 S. Erbas-Cakmak, D. A. Leigh, C. T. McTernan and A. L. Nussbaumer, *Chem. Rev.*, 2015, **115**, 10081–10206.
4 W.-Y. Gao, M. Chrzanowski and S. Ma, *Chem. Soc. Rev.*, 2014, **43**, 5841–5866.
5 S. Singh, A. Aggarwal, N. V. S. D. K. Bhupathiraju, G. Arianna, K. Tiwari and C. M. Drain, *Chem. Rev.*, 2015, **115**, 10261–10306.
6 R. Paolesse, S. Nardis, D. Monti, M. Stefanelli and C. Di Natale, *Chem. Rev.*, 2017, **117**, 2517–2583.
7 H. Lu and N. Kobayashi, *Chem. Rev.*, 2016, **116**, 6184–6261.
8 V. Borovkov, *Symmetry*, 2014, **6**, 256–294.
9 G. A. Hembury, V. V. Borovkov and Y. Inoue, *Chem. Rev.*, 2008, **108**, 1–73.
10 V. V. Borovkov and Y. Inoue, in *Supramolecular Chirality*, ed. M. Crego-Calama and D. N. Reinhoudt, Springer Berlin Heidelberg, Berlin, Heidelberg, 2006, pp. 89–146.
11 P. Liu, P. Neuhaus, D. V. Kondratuk, T. S. Balaban and H. L. Anderson, *Angew. Chem., Int. Ed.*, 2014, **53**, 7770–7773.
12 T. Mizutani, T. Ema, T. Yoshida, Y. Kuroda and H. Ogoshi, *Inorg. Chem.*, 1993, **32**, 2072–2077.
13 H. Ogoshi and T. Mizutani, *Acc. Chem. Res.*, 1998, **31**, 81–89.
14 M. Balaz, M. D. Napoli, A. E. Holmes, A. Mammana, K. Nakanishi, N. Berova and R. Purrello, *Angew. Chem., Int. Ed.*, 2005, **44**, 4006–4009.
15 A. D'Urso, P. F. Nicotra, G. Centonze, M. E. Fragalà, G. Gattuso, A. Notti, A. Pappalardo, S. Pappalardo, M. F. Parisi and R. Purrello, *Chem. Commun.*, 2012, **48**, 4046–4048.
16 A. D'Urso, N. Marino, M. Gaeta, M. S. Rizzo, D. A. Cristaldi, M. E. Fragalà, S. Pappalardo, G. Gattuso, A. Notti, M. F. Parisi, I. Pisagatti and R. Purrello, *New J. Chem.*, 2017, **41**, 8078–8083.
17 E. Bellacchio, R. Lauceri, S. Gurrieri, L. M. Scolaro, A. Romeo and R. Purrello, *J. Am. Chem. Soc.*, 1998, **120**, 12353–12354.
18 R. Lauceri, A. Raudino, L. M. Scolaro, N. Micali and R. Purrello, *J. Am. Chem. Soc.*, 2002, **124**, 894–895.
19 R. Lauceri, G. F. Fasciglione, A. D'Urso, S. Marini, R. Purrello and M. Coletta, *J. Am. Chem. Soc.*, 2008, **130**, 10476–10477.
20 G. D. Luca, A. Romeo, L. M. Scolaro and R. F. Pasternack, *Chem. Commun.*, 2010, **46**, 389–391.
21 I. Occhiuto, G. D. Luca, V. Villari, A. Romeo, N. Micali, R. F. Pasternack and L. M. Scolaro, *Chem. Commun.*, 2011, **47**, 6045–6047.
22 I. G. Occhiuto, M. Samperi, M. Trapani, G. De Luca, A. Romeo, R. F. Pasternack and L. M. Scolaro, *J. Inorg. Biochem.*, 2015, **153**, 361–366.
23 M. Gaeta, D. Raciti, R. Randazzo, C. M. A. Gangemi, A. Raudino, A. D'Urso, M. E. Fragalà and R. Purrello, *Angew. Chem., Int. Ed.*, 2018, **57**, 10656–10660.
24 R. Randazzo, A. Mammana, A. D'Urso, R. Lauceri and R. Purrello, *Angew. Chem., Int. Ed.*, 2008, **47**, 9879–9882.
25 R. Aav, E. Shmatova, I. Reile, M. Borissova, F. Topić and K. Rissanen, *Org. Lett.*, 2013, **15**, 3786–3789.
26 M. Öeren, E. Shmatova, T. Tamm and R. Aav, *Phys. Chem. Chem. Phys.*, 2014, **16**, 19198–19205.
27 E. Prigorchenko, M. Öeren, S. Kaabel, M. Fomitšenko, I. Reile, I. Järving, T. Tamm, F. Topić, K. Rissanen and R. Aav, *Chem. Commun.*, 2015, **51**, 10921–10924.
28 S. Kaabel, J. Adamson, F. Topić, A. Kiesilä, E. Kalenius, M. Öeren, M. Reimund, E. Prigorchenko, A. Lõokene, H. J. Reich, K. Rissanen and R. Aav, *Chem. Sci.*, 2017, **8**, 2184–2190.
29 N. N. Andersen, M. Lisbjerg, K. Eriksen and M. Pittelkow, *Isr. J. Chem.*, 2018, **58**, 435–448.
30 H.-J. Buschmann, A. Zielesny and E. Schollmeyer, *J. Inclusion Phenom. Macrocyclic Chem.*, 2006, **54**, 181–185.
31 M. Singh, E. Solel, E. Keinan and O. Reany, *Chem. – Eur. J.*, 2015, **21**, 536–540.
32 M. Lisbjerg, B. M. Jessen, B. Rasmussen, B. E. Nielsen, A. Ø. Madsen and M. Pittelkow, *Chem. Sci.*, 2014, **5**, 2647–2650.
33 T.-L. Teo, M. Vetrichelvan and Y.-H. Lai, *Org. Lett.*, 2003, **5**, 4207–4210.
34 B. P. Borah and J. Bhuyan, *J. Chem. Sci.*, 2018, **130**, 117.
35 Y. Gao, X. Zhang, C. Ma, X. Li and J. Jiang, *J. Am. Chem. Soc.*, 2008, **130**, 17044–17052.
36 B. M. J. M. Suijkerbuijk, D. M. Tooke, A. L. Spek, G. van Koten and R. J. M. Klein Gebbink, *Chem. – Asian J.*, 2007, **2**, 889–903.
37 J. Bhuyan and S. Sarkar, *Cryst. Growth Des.*, 2011, **11**, 5410–5414.
38 C. K. Schauer, O. P. Anderson, S. S. Eaton and G. R. Eaton, *Inorg. Chem.*, 1985, **24**, 4082–4086.
39 M. Schmittel and S. K. Samanta, *J. Org. Chem.*, 2010, **75**, 5911–5919.
40 L. Favereau, A. Cnossen, J. B. Kelber, J. Q. Gong, R. M. Oetterli, J. Cremers, L. M. Herz and H. L. Anderson, *J. Am. Chem. Soc.*, 2015, **137**, 14256–14259.
41 F. Ulatowski, K. Dąbrowa, T. Bałakier and J. Jurczak, *J. Org. Chem.*, 2016, **81**, 1746–1756.
42 P. Thordarson, *Chem. Soc. Rev.*, 2011, **40**, 1305–1323.
43 D. B. Hibbert and P. Thordarson, *Chem. Commun.*, 2016, **52**, 12792–12805.
44 E. Prigorchenko, S. Kaabel, T. Narva, A. Baškir, M. Fomitšenko, J. Adamson, I. Järving, K. Rissanen, T. Tamm and R. Aav, *Chem. Commun.*, 2019, **55**, 9307–9310.